2

The Origin and Evolution of Saturn, with Exoplanet Perspective

SUSHIL K. ATREYA, AURÉLIEN CRIDA, TRISTAN GUILLOT, JONATHAN I. LUNINE, NIKKU MADHUSUDHAN AND OLIVIER MOUSIS

Abstract

Saturn formed beyond the snow line in the primordial solar nebula, and that made it possible for it to accrete a large mass. Disk instability and core accretion models have been proposed for Saturn's formation, but core accretion is favored on the basis of its volatile abundances, internal structure, hydrodynamic models, chemical characteristics of protoplanetary disk, etc. The observed frequency, properties, and models of exoplanets provide additional supporting evidence for core accretion. The heavy elements with mass greater than ^{4}He make up the core of Saturn, but are presently poorly constrained, except for carbon. The C/H ratio is super-solar, and twice that in Jupiter. The enrichment of carbon and other heavy elements in Saturn and Jupiter requires special delivery mechanisms for volatiles to these planets. In this chapter we will review our current understanding of the origin and evolution of Saturn and its atmosphere, using a multifaceted approach that combines diverse sets of observations on volatile composition and abundances, relevant properties of the moons and rings, comparison with the other gas giant planet, Jupiter, and analogies to the extrasolar giant planets, as well as pertinent theoretical models.

2.1 Introduction

Saturn, though about one-third the mass of Jupiter, is the largest planetary system in the solar system, considering the vast reach of its rings and dozens of known moons. Thus, Saturn is key to understanding the origin and evolution of the solar system itself. Models, observations, comparison with Jupiter, the other gas giant planet, and analogies with extrasolar giant planets have begun to give a sense of how Saturn, in particular, and the giant planets in general, originated and evolved.

Two distinct mechanisms of giant planet formation have been proposed in the literature: (1) disk instability and (2) nucleated instability (or core accretion). The latter goes back to papers by Hayashi (1981) and his colleagues (e.g. Mizuno 1980), and requires the accretion of a solid body (rock/metal, ice, and, possibly, refractory organics) up to a critical mass threshold at which rapid accretion of gas becomes inevitable – typically 10 times the mass of the Earth (see Armitage 2010, for a discussion). The former theory had its origin in the 1970s (see Cameron 1979) for hot, massive disks, but it was determined later (Boss 2000; Mayer et al. 2002) that the instabilities required to break up a portion of a gaseous disk into clumps are a feature of cold, massive disks. We will focus on each of these contrasting models in turn, and then discuss the observational indicators in our own and extrasolar planetary systems that might distinguish between the two models.

The disk instability model is based on numerical simulations showing that massive, relatively cold disks will spontaneously fragment due to a gravitational instability, leading to multiple discrete, self-gravitating masses. In computer simulations of the process these features seem somewhat ill defined, and it is not possible to track the subsequent condensation of these features in the same hydrodynamical simulation that tracks the onset of the instability itself.

Nonetheless, basic disk physics dictates that such fragmentation will occur for a sufficiently massive or cold disk (Armitage 2010) and that the timescale for the fragmentation, once the instability does occur, is extremely short – hundreds to thousands of years.

Once formed, the fragments (assuming they continue to contract to form giant planets) are usually sufficiently numerous that the aggregate planetary system is dynamically unstable. The planets will gravitationally interact, scattering some out of the system and leaving the others in a variety of possible orbits. The evidence from microlensing of a substantial population of free-floating Jupiter-mass objects (Sumi et al. 2011) not associated with a parent star constitutes one argument in favor of the importance of this formation mechanism.

On the other hand, it is not evident how giant planets formed by the disk instability mechanism acquire significant amounts of heavy elements over and above their parent star's abundances. It has been argued that subsequent accretion of planetesimals would generate the increased metallicity, but the disruption of the disk associated with the gravitational instability might have removed the raw material for large amounts of planetesimals – the materials going into numerous giant planets that are then kicked out of the system. A subsequent phase of disk building or direct accretion of planetesimals from the surrounding molecular cloud may have to be invoked. And this begs the question of core formation – giant planets formed in this way may have super-solar metallicities but lack a heavy element core unless (as seems unlikely) very large (Earth-sized) planets are consumed by these objects.

The core accretion model, in contrast, begins by building a heavy element core through planetesimal and embryo accretion in the gaseous disk (embryo is usually reserved for lunar-sized bodies and upward). At some point, the gravitational attraction of the large core leads to an enhanced accretion of gas, so much so that gas accretion quickly dominates in a runaway process and the object gains largely nebular-composition gas until its mass is large enough to create a gap in the disk and slow accretion. Such a model produces, by definition, a heavy element core, and through co-accretion of gas and planetesimals, an envelope enrichment of heavy elements as well. The model's Achilles heel is the time required to build the heavy element core to the point where rapid gas accretion occurs – millions of years or more. The onset of rapid gaseous accretion, by which point further growth may be rapid, depends not only on the core accretion rate but also, through the critical core mass (roughly 10 M_E, where M_E is an Earth mass) needed to trigger rapid gas accretion, the envelope opacity, and hence metallicity. Furthermore, the core accretion rate itself is a sensitive function of what one assumes about the planetesimal size distribution and surface density in the disk.

A plausible timescale for the formation of Saturn must be consistent with the lifetime of gas in disks, but may also be constrained by the 3–5 million-year (Myr) estimate of the formation duration of Iapetus, from its geophysical shape and thermal history (Castillo-Rogez et al. 2009). Earliest models had lengthy formation times (e.g. 8 Myr; Pollack et al. 1996), but more recent models can make Saturn in a few million years by appropriate selection of nebular parameters such as grain distribution and opacity (Dodson-Robinson et al. 2008).

The overall history of the solar system and presence of a substantial terrestrial planet system inward of Jupiter and Saturn suggests that the extreme dynamical scattering suffered after disk instability protoplanets are formed did not happen in our solar system. Furthermore, if the 3–5-million-year estimate of the interval between the formation of the first solids and the formation of Iapetus (Castillo-Rogez et al. 2009) is correct, the disk instability – if it occurred – would have produced Saturn much too soon after (or even before) the first solids in the solar system condensed out. There is sufficient evidence that the first solids, millimeter-sized chondrules and calcium aluminum inclusions (CAIs) in chondrites, date back to 4.5682 Gyr (billion years) (Amelin et al. 2010), which provides clear evidence that submicron-sized interstellar grains were sticking and accumulating to form solids at the very beginning of the solar system.

Measurement by the Juno mission of the water abundance below the meteorology layer in Jupiter, tied to the abundances of other major elements measured by the Galileo probe, will also provide an indication of how much planetesimal material was accreted (Helled and Lunine 2014), and to some extent, the nature of the carrier species (e.g. Mousis 2012). Although it is possible to enrich the envelopes of the giant planets even in

the disk instability model by adding planetesimals much later, the presence of both a substantial (10 M_E) core and envelope enrichment of heavy elements would strongly militate in favor of the core accretion model. Saturn's core mass may be measured by Cassini, but an inventory of the envelope enrichment of heavy elements and measurement of the deep water abundance will have to await a future Saturn probe.

The core accretion model gets a boost also from observational surveys of exoplanets. An analysis of the frequency of planets with different masses, sizes, orbits, and host characteristics reveals that a greater percentage of giant planets are found around higher-metallicity stars, and smaller planets between Earth's and Neptune's mass far exceed Jupiter-sized planets (Howard 2013; Johnson et al. 2010). This is what one would expect if core accretion were prerequisite for planetary formation. Thus, for our planetary system, at least, core accretion seems to make more sense. Trying to constrain detailed formation mechanisms by matching orbital properties is much more difficult because of the profound effects of migration (Mordasini, et al. 2009; Ida et al. 2013 and references therein).

In addition to their occurrence rates and orbital characteristics, the masses, radii, and atmospheric volatile gas compositions of giant exoplanets may also provide important clues regarding their formation processes, and in turn, formation of Saturn and Jupiter in the solar system. With rapid advances in spectroscopic observations of exoplanets, a number of gases relevant to formation models, including water vapor, methane and carbon monoxide have been detected in several giant exoplanets (Section 2.5), revealing diversity in chemical abundances. For example, there are some planets (e.g. HD 209458b) with seemingly lower H_2O abundances than expected from solar elemental composition (e.g. Deming et al. 2013; Madhusudhan et al. 2011a, 2014a), while others (e.g. WASP-43b) appear consistent with super-solar H_2O (e.g. Kreidberg et al. 2014). The latter is consistent with super-solar abundance of measured heavy elements in Saturn and Jupiter (Section 2.2.1), with a good likelihood that their original cores were rich in water ice. On the other hand, WASP-12b – which indicates a C/O ratio (≥1) twice solar (~0.5) – argues for a core made up of largely carbon-bearing constituents. If this result is confirmed for a multitude of similar exoplanets, it would have important implications for their formation and the formation of the gas giant planets of the solar system. More generally, new theoretical studies are suggesting that the observable O/H, C/H, and, hence, C/O ratios in giant exoplanetary atmospheres can place powerful constraints on their formation and migration mechanisms, as discussed in Section 2.5.3.

2.2 Observational Constraints

The models of Saturn's formation and evolution are constrained by data presently available on the planet's chemical composition and its interior. This section elaborates on each of these aspects and forms the basis for the discussions in subsequent sections.

2.2.1 Elemental Composition of Saturn's Atmosphere and Comparison to Jupiter

The composition of Saturn's atmosphere has been measured by remote sensing from ground-based and Earth-orbiting telescopes and flyby and orbiting spacecraft for over half a century. These observations have been instrumental in revealing the chemical makeup of Saturn's stratosphere and upper troposphere. As a result, mole fractions of helium (He), methane (CH_4), and a number of its photochemical products including methyl radical (CH_3), ethane (C_2H_6), acetylene (C_2H_2), methyl acetylene (C_3H_4), and benzene (C_6H_6), ammonia (NH_3), hydrogen sulfide (H_2S), and those species that are in thermochemical disequilibrium in Saturn's upper troposphere and stratosphere such as phosphine (PH_3), carbon monoxide (CO), germane (GeH_4), and Arsine (AsH_3) have been measured to varying degrees of precision. Some of the most precise data have come from observations made by the Cassini spacecraft (Fletcher et al., this book) that attained orbit around Saturn in 2004 and will embark on proximal orbits toward the end of the mission in 2017 (Baines et al., this book).

The abundances of certain heavy elements (m/z $>^4$He) and their isotopes can be derived from their principal chemical reservoirs in the atmosphere. As discussed earlier, heavy elements are key to constraining the models of the formation of Saturn and its atmosphere. Current best data on the abundances of elements relative to hydrogen in Saturn are listed in

Table 2.1. As Jupiter, the other gas giant planet in the solar system, is a good analog for Saturn, we list for comparison also the elemental abundances in Jupiter's atmosphere.

Many more heavy elements have been determined at Jupiter, in contrast to Saturn, because of in situ Galileo Jupiter entry probe measurements from 1995. Enrichment factors of the elements relative to protosolar values are also listed in Table 2.1, using currently available solar elemental abundances from two different sources (Asplund et al. 2009; Lodders et al. 2009). Further insight into key elemental abundances is given below, and the reader is referred also to the table footnotes.

After hydrogen, helium is the most abundant element in the universe, the sun, and the giant planets. Conventional thinking has been that the current abundance of helium ratioed to hydrogen in the giant planets should be the same as in the primordial solar nebula from which these planets formed, and originally the Big Bang, in which helium was created. Thus, precise determination of the helium abundance is essential to understanding the formation of the giant planets, in particular, and to shedding light on the solar nebula and the universe in general. Whereas helium has been measured very accurately at Jupiter by two independent techniques on the Galileo probe (Table 2.1), such is not the case for Saturn. In the absence of an entry probe at Saturn, helium abundance at Saturn was derived from atmospheric mean molecular weight (μ), using a combination of the Voyager infrared spectrometer (IRIS) and the radio science (RSS) investigations. RSS measured radio refractivity that provides the information on T/μ, where T is the temperature measured by both instruments.

Initial analysis using the IRIS-RSS data (Conrath et al. 1984) yielded a greatly sub-solar He/H=0.017 ±0.012 (He/H_2=2×He/H). Subsequent reanalysis of the data employing IRIS alone gave He/H between 0.055 and 0.08 (Conrath and Gautier 2000). The authors emphasize, however, the retrieval of He/H is non-unique, but strongly suggests a value significantly greater than the earlier result that was based on the combined IRIS-RSS approach. For the purpose of this chapter, we take an average of the range of Saturn's He/H of 0.055–0.08, and express it as 0.0675±0.0125 (Table 2.1), but with the caveat that the value could well change following detailed analysis of the Cassini CIRS data and, especially, future in situ measurements at Saturn, as did Jupiter's He/H_2 following in situ measurements by the Galileo probe compared to the value derived from Voyager's remote sensing observations. The current estimate of He/H in Saturn's upper troposphere is about 0.7× solar compared to Jupiter's 0.8× solar. The sub-solar He/H_2 in the tropospheres of Jupiter and Saturn presumably results from the removal of some fraction of helium vapor through condensation as liquid at 1–2 megabar pressure in the interiors of these planets, followed by separation of helium droplets from metallic hydrogen. The severe depletion of Ne observed by the Galileo probe (Table 2.1) in Jupiter is excellent evidence of the helium-hydrogen immiscibility layer, as helium droplets absorb neon vapor, separate from hydrogen, rain toward the core, and this results in the depletion of helium and neon in the upper troposphere (Roulston and Stevenson 1995; Wilson and Militzer 2010). Models predict that the cooler interior of Saturn is expected to result in a greater degree of helium condensation and therefore a tropospheric He/H_2 ratio lower for Saturn than for Jupiter. Although the central value for Saturn is smaller than Jupiter's, the large uncertainty of Saturn's result does not provide a definite answer. Helium differentiation in Saturn's interior is invoked also as a way to explain the planet's large energy balance (Conrath et al. 1989). Without such chemical differentiation, models predict the heat flux excess at Saturn to be about three times lower than observed (Grossman et al. 1980), but the equation of state for the high-pressure, high-temperature interior is uncertain, so the modeled excess is not that well constrained (see Chapter 3 by Fortney et al. for additional details). Saturn and Jupiter both emit nearly twice the thermal radiation compared to the radiation the absorb from the sun. Whereas the release of heat of accretion from conversion of the gravitational potential energy as these planets cool and contract over time accounts for a good fraction of the energy balance of Jupiter, helium differentiation may play a significant role at Saturn. Since helium is denser than hydrogen, gravitational potential energy available for conversion to heat increases as helium raindrops begin to separate from hydrogen and precipitate upon reaching centimeter size. In summary, there are indications that helium is depleted relative to solar in Saturn's

Table 2.1 *Elemental Abundances in Jupiter and Saturn and Ratios to Protosolar Values*

Elements	Jupiter	Saturn	Sun-Protosolar (Asplund et al. 2009) [a,b]	Jupiter/ Protosolar (using Asplund et al. 2009) [a,b]	Saturn/Protosolar (using Asplund et al. 2009) [a,b]	Sun-Protosolar (Lodders et al. 2009) [m]	J P (e
He/H	$7.85 \pm 0.16 \times 10^{-2}$ [c]	$5.5–8.0 \times 10^{-2}$ [i], taken as $6.75 \pm 1.25 \times 10^{-2}$	9.55×10^{-2}	0.82 ± 0.02	0.71 ± 0.13 (?)	9.68×10^{-2}	0
Ne/H	$1.24 \pm 0.014 \times 10^{-5}$ [d]		9.33×10^{-5}	0.13 ± 0.001		1.27×10^{-4}	0
Ar/H	$9.10 \pm 1.80 \times 10^{-6}$ [d]		2.75×10^{-6}	3.31 ± 0.66		3.57×10^{-6}	2
Kr/H	$4.65 \pm 0.85 \times 10^{-9}$ [d]		1.95×10^{-9}	2.38 ± 0.44		2.15×10^{-9}	2
Xe/H	$4.45 \pm 0.85 \times 10^{-10}$ [d]		1.91×10^{-10}	2.34 ± 0.45		2.1×10^{-10}	2
C/H	$1.19 \pm 0.29 \times 10^{-3}$ [e]	$2.65 \pm 0.10 \times 10^{-3}$ [j]	2.95×10^{-4}	4.02 ± 0.98	8.98 ± 0.34	2.77×10^{-4}	4
N/H	$3.32 \pm 1.27 \times 10^{-4}$ [e]	$0.80–2.85 \times 10^{-4}$ [k];	7.41×10^{-5}	4.48 ± 1.71[e]	1.08–3.84;	8.19×10^{-5}	4
	$4.00 \pm 0.50 \times 10^{-4}$ [f]	$2.27 \pm 0.57 \times 10^{-4}$ with		5.40 ± 0.68[f]	3.06 ± 0.77 with		4
	$2.03 \pm 0.46 \times 10^{-4}$ [g]	$f\mathrm{NH_3}=4 \pm 1 \times 10^{-4}$		2.70 ± 0.60[g]	$f\mathrm{NH_3}=4 \pm 1 \times 10^{-4}$		2
O/H	$2.45 \pm 0.80 \times 10^{-4}$ [e]		5.37×10^{-4}	0.46 ± 0.15 (hotspot)		6.07×10^{-4}	0 (l
S/H	$4.45 \pm 1.05 \times 10^{-5}$ [e]	1.88×10^{-4} [l]	1.45×10^{-5}	3.08 ± 0.73	13.01	1.56×10^{-5}	2
P/H	$1.08 \pm 0.06 \times 10^{-6}$ [h]	$3.64 \pm 0.24 \times 10^{-6}$ [h]	2.82×10^{-7}	3.83 ± 0.21	12.91 ± 0.85	3.26×10^{-7}	3

[a] Protosolar values calculated from the solar photospheric values of Asplund et al. (2009, table 1).
[b] According to Asplund et al. (2009), the protosolar metal abundances relative to hydrogen can be obtained from the present-day photos et al. 2009) increased by +0.04 dex, i.e. ~11%, with an uncertainty of ±0.01 dex; the effect of diffusion on He is very slightly larger: +0.0 et al. (2005, 2007) used the same correction of +0.05 dex for all elements (dex stands for "decimal exponent," so that 1 dex=10).
[c] von Zahn et al. (1998), using helium detector on Galileo Probe; independently confirmed by the Galileo Probe Mass Spectrometer (G
[d] Mahaffy et al. (2000); Kr and Xe represent the sum of all isotopes except for ^{126}Xe and ^{124}Xe that could not be measured by the GPM together they make up 0.2% of the total xenon in the sun.

(e) Wong et al. (2004), based on re-calibration of the GPMS data on CH_4, NH_3, H_2O, and H_2S down to 21 bars, using an experiment un values reported in Niemann et al. (1998) and Atreya et al. (1999, 2003).

(f) Folkner et al. (1998), by analyzing the attenuation of the Galileo probe-to-orbiter radio communication signal (L-band at 1387 MH Jupiter's atmosphere.

(g) Juno microwave radiometer (MWR) preliminary result in the equatorial region and two different longitudes (Bolton et al. 2017).

(h) Fletcher et al. (2009a) derived global PH_3 mole fractions of 1.86±0.1 ppm and 6.41±0.42 ppm, respectively, in the upper troposphe an analysis of the mid-IR emission measured by the Cassini Composite Infrared Spectrometer (CIRS).

(i) Conrath and Gautier (2000) give a range of 0.11–0.16 for the He/H_2 mole fraction from re-analysis of the Voyager IRIS data at Saturn use an average He/H=0.0675 for the purpose of calculating the ratios of other elements relative to hydrogen in Saturn.

(j) Fletcher et al. (2009b) report mole fraction of $CH_4=4.7\pm0.2\times10^{-3}$ from an analysis of the CIRS data.

(k) Fletcher et al. (2011), using VIMS data giving an ammonia mole fraction, fNH_3, in the 1–3 bar region that is 140±50 ppm (scatter scattering) and rises to 300–500 ppm at the equator. If the maximum in ammonia measured at the equator (300–500 ppm, or 400± atmospheric NH_3, the corresponding $NH_3/H = 2.27\pm0.6\times10^{-4}$.

(l) Briggs and Sackett (1989), using the VLA and the Arecibo microwave and radio data. The authors reported 10× solar H_2S, using sol current listing (Cameron 1982). The S/H result is questionable (see text).

(m) Protosolar values based on present-day solar photospheric values of Lodders et al. (2009, table 4). The proto-solar abundances are ca values using the following corrections: +0.061 dex for He and +0.053 dex for all other elements.

troposphere, but the extent of such depletion will continue to be a subject of debate until precise in situ measurements can be made. In this regard, the final proximal orbits of Cassini in September 2017 are promising for the measurement of helium by the Ion and Neutral Mass Spectrometer down to ~1700 km or ≤0.1 nanobar (S. Edgington, personal comm., 2015), which is above Saturn's homopause level (1000–1100 km, or ~10–100 nanobar; Atreya 1986; Strobel et al., this book), and perhaps deeper in the final trajectory when the spacecraft plunges into Saturn. Extrapolation to a well-mixed troposphere would be model dependent even if the homopause level could be derived independently from the Cassini occultation data in the proximal orbits. Hence, precise helium abundance measurement directly in the well-mixed troposphere will still be essential, and that can only be done from an entry probe.

The nitrogen elemental abundance in Saturn is obtained from Saturn's principal nitrogen-bearing molecule, NH_3. From an analysis of the Cassini Visual and Infrared Mapping Spectrometer (VIMS) data, Fletcher et al. (2011) derive an ammonia mole fraction, $f NH_3$, in the 1–3 bar region that is 140±50 ppm (scattering), 200±80 ppm (non-scattering), and rising to 300–500 ppm at the equator. If we assume that maximum in ammonia measured at the equator (300–500 ppm, taken as $4\pm1\times10^{-4}$ here) represents also the NH_3 mole fraction in Saturn's deep well-mixed troposphere, then the corresponding $NH_3/H = 2.27\pm0.6\times10^{-4}$. That would imply an N/H enrichment of about 3× solar at Saturn, in contrast to Jupiter's roughly 3–5× solar. Previously, de Pater and Massie (1985) also found a 3× solar enhancement in Saturn's N/H in the 3-bar region, based on the VLA observations. The VLA and the Cassini RADAR 2.2 cm data (Laraia et al. 2013) also show that ammonia is subsaturated down to several bars, which most likely results from the loss of NH_3 in the lower clouds of NH_4SH (or another form such as $(NH_4)_2S$) at ≥5 bars and the NH_3-H_2O (aqueous-ammonia) solution cloud between approximately 10 and 20 bars, depending on the enhancement of O/H (H_2O) above solar (Atreya et al. 1999; Atreya and Wong 2005; see also Section 2.6 and Figure 2.9 therein). Whether the above 3× solar N/H in the 3-bar region is representative of the true nitrogen elemental ratio in Saturn's deep well-mixed troposphere is presently an open question, as the infrared or radio data can neither confirm it nor rule it out. Unlike Saturn, there is no such ambiguity in the determination of Jupiter's N/H, since direct in situ measurements of NH_3 could be made by the Galileo probe mass spectrometer (GPMS; Niemann et al. 1998) down to 21 bars, which is well below the expected NH_3 condensation level of 0.5–1 bar. Independently, NH_3 was derived also by analyzing the attenuation of the Galileo probe-to-orbiter radio communication signal (L-band at 1387 MHz or 21.6 cm) by ammonia in Jupiter's atmosphere (Folkner et al. 1998). NH_3 from the two sets of data agree to within 20%, with tighter constraints coming from the radio attenuation data, which yields N/H = 5.40±0.68× solar (Table 2.1). It is generally assumed the Galileo probe value is likely representative of the global N/H in Jupiter, as the measurements were done well below any possible traps of ammonia, including condensation clouds of NH_3, NH_4SH, and NH_3-H_2O. Preliminary deep NH_3 values from the Juno microwave radiometer (Bolton et al. 2017) overlap the Galileo mass spectrometer value within the range of uncertainty of the two datasets, but not the Galileo radio attenuation data (Table 2.1). At Saturn, NH_3 from remote sensing extends to ~3 bars; however, an entry probe to deeper levels can answer whether that value is representative of the global well-mixed N/H or similar to C/H.

Sulfur is sequestered largely in the H_2S gas in the atmospheres of Jupiter and Saturn. Whereas Jupiter's H_2S could be measured directly and precisely in situ by the Galileo probe (Table 2.1), it was derived indirectly at Saturn by fitting the VLA and Arecibo microwave and radio data to assumed NH_3 abundances (Briggs and Sackett 1989). Although direct microwave absorption by H_2S could not be measured in these observations, they deduced H_2S by analyzing NH_3, whose abundance is controlled to some extent by H_2S, since models predict it would remove a portion of the NH_3 vapor via the formation of an NH_4SH cloud below. Using the then-available solar $S/H=1.88\times10^{-5}$ (Cameron 1982), they derived a 10× solar enrichment of S/H in Saturn's atmosphere, which translates into 12–13× solar S/H using current solar S/H values, or about four times the value determined by the Galileo probe in Jupiter (Table 2.1). It is important to add a caveat, however. Whereas the Jupiter result comes from direct, in situ

measurement of H_2S, the above result for Saturn is highly model-dependent, as it depends on the assumption of the formation of purported NH_4SH cloud whose thermochemical properties are poorly constrained. Since sulfur is a key heavy element in the models of Saturn's formation, a fresh set of data on Saturn's H_2S is warranted.

We list P/H in Table 2.1, but add a caveat that it may not represent the true P/H value in the deep well-mixed atmospheres of Jupiter or Saturn. This is because PH_3, the principal reservoir of phosphorus in the atmospheres of Jupiter and Saturn, is a disequilibrium species that is thermochemically stable in the deep atmosphere at pressures of about one thousand bars where the temperature is ~1000 K or greater (Fegley and Prinn 1985; Visscher and Fegley 2005), but it could only be measured in the upper troposphere/lower stratosphere. As PH_3 is dredged up from deep in the atmosphere to the upper atmosphere, it may potentially undergo loss due to oxidation to P_4O_6 by water vapor and solution in any water clouds along the way, or by other chemical reactions. Thus, the P/H ratio deduced from observations of PH_3 for Saturn and Jupiter in the upper atmosphere may represent a lower limit to the P/H ratio in their deep well-mixed atmosphere. Hence, the P/H values listed in Table 2.1 should not automatically be taken as a good proxy for the enrichment of other heavy elements not yet measured in Jupiter or Saturn. On the other hand, disequilibrium species such as PH_3, GeH_4, AsH_3, and CO are excellent tracers of the strength of convective mixing in the deep atmospheres of Saturn and Jupiter, and some could potentially be exploited to yield also a rough estimate of the deep water abundance.

Oxygen is arguably the most crucial of all heavy elements for constraining the formation models of Jupiter and Saturn. This is because in the reducing environments of the giant planets, oxygen is predominantly sequestered in water, which was presumably the original carrier of the heavy elements that formed the core and made it possible to accrete gas and complete the planet formation. (CO is another oxygen bearing species, but is a million times less abundant than water.) Yet the deep well-mixed abundance of water, and hence of O/H, remains a mystery. In the case of Jupiter, the Galileo probe entered an anomalously dry region known as a 5-micron hot spot. In this "Sahara Desert of Jupiter," water was found to be severely depleted (Niemann et al. 1998; Atreya et al. 1999, 2003). Although the probe mass spectrometer measured water vapor down to 21 bars, i.e. well below the expected condensation level of H_2O between 5 and 10 bars, it was still sub-solar at that level (Table 2.1), but rising. The determination of Jupiter's water abundance must await the analysis of Juno microwave radiometer observations in 2016–2017. No measurements of water vapor are available for Saturn's troposphere, however. The presence of water in Saturn's atmosphere is inferred indirectly from observations of visible lightning by Cassini's imaging spectrometer where lightning storms were predicted by Cassini's radio observations (Dyudina et al. 2010). Broadband clear filter observations showed visible lightning at ~35°S on the nightside in 2009 (Dyudina et al. 2010) and in blue wavelengths only on the dayside in the 2010–2011 giant lightning storm at ~35°N (Dyudina et al. 2013). These authors conjecture that a 5- to 10-times enhancement of water over solar can explain Saturn's lower occurrence rate for moist convection, an indicator of lightning, compared to Jupiter's (Dyudina et al. 2010). Similarly, using thermodynamic arguments Li and Ingersoll (2015) conclude that Saturn's quasi-periodic giant storms, which recur every few decades, result from interaction between moist convection and radiative cooling above the water cloud base, provided that the tropospheric water vapor abundance is 1 or greater, i.e. O/H $\geq$10× solar. Such an enrichment in O/H would result in a droplet cloud of NH_3-H_2O at ~20-bar level at Saturn (Atreya and Wong 2005; see also section 2.6 and figure 2.9 therein). Although direct measurements of Saturn's well-mixed water may have to wait for future missions, as discussed in Section 2.5, the recent discoveries of hot giant exoplanets and a Saturn-analog exoplanet are making it possible to measure H_2O abundances in their atmospheres, and in turn informing possible H_2O abundances in solar system giant planets.

Highly precise measurements of methane in the atmosphere of Saturn have been carried out with Cassini's composite infrared spectrometer (CIRS) instrument (Flasar et al. 2005), which yield a mole fraction of $CH_4 = 4.7\pm0.2\times10^{-3}$ (Fletcher et al. 2009b). This results in a robust determination of the C/H ratio in Saturn (about twice the Jupiter value) that can be compared with rather imprecise but definitely

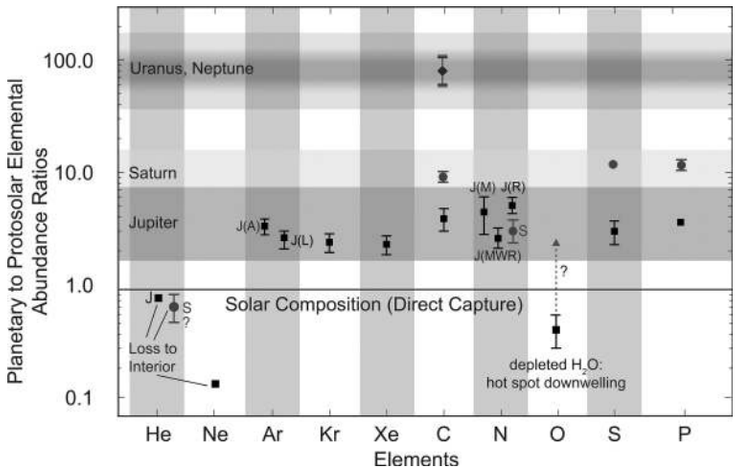

Figure 2.1 Abundances of key elements in the atmospheres of Saturn (brown dots, and label S) and Jupiter (black squares) relative to protosolar values derived from the present-day photospheric values of Asplund et al. (2009). Only C/H is presently determined for Uranus and Neptune, though poorly; its best estimate from Earth-based observations is shown. The values are listed in Table 2.1. All values are ratioed to H (multiply by 2 for ratio to H_2). Direct gravitational capture would result in solar composition, i.e. no volatile enrichment, hence they would all fall on the horizontal line (normalized to solar) in the middle of the figure. Only He, C, N, S, and P have been determined for Saturn, but only C/H is robust for the well-mixed atmosphere (see text). The Jupiter values are from the Galileo probe mass spectrometer (GPMS), except for N/H from NH_3 that was measured on the Galileo probe by the GPMS [J(M)] and from attenuation of the probe radio signal through the atmosphere [J(R)] as well as Juno microwave radiometer [J(MWR)], whose preliminary result is shown. For Ar, enrichments using both Asplund et al. [J(A)] and Lodders et al. [J(L)] solar values are shown. O/H is sub-solar in the very dry entry site of the Galileo Probe at Jupiter, but was still on the rise at the deepest level probed. Helium is depleted in the shallow troposphere due to condensation and differentiation in the planetary interior. Ne was also depleted in Jupiter as neon vapor dissolves in helium droplets. (A black-and-white version of this figure appears in some formats. For the color version, please refer to the plate section.)

higher estimates of C/H in Uranus and Neptune, as a way of constraining the giant planet formation scenarios.

Heavy noble gases, Ne, Ar, Kr, and Xe, have been measured only in Jupiter's atmosphere (Table 2.1), since they can only be detected in situ by an entry probe, not by remote sensing. As noble gases are chemically inert, their abundance is unaffected by chemistry and condensation processes that control NH_3, H_2S, H_2O, and PH_3. Thus, the heavy noble gas enrichments are expected to be the same everywhere in the atmosphere. At Jupiter, with the exception of neon, they range from a factor of 2 to 3× solar within the range of uncertainty of their planetary measurements and the solar values (Table 2.1). As neon dissolves in liquid helium, it is removed along with helium, which condenses in the 3 megabar region in Jupiter's interior, and is thus found depleted at observable shallow tropospheric levels (Wilson and Militzer 2010). At Saturn, neon is expected to meet the same fate.

Figure 2.1 shows the enrichment factors of the heavy elements and He in the atmospheres of Saturn and Jupiter relative to their protosolar values (all ratioed to H). Here we use the Asplund et al. (2009) compilation of photospheric elemental abundances (their table 1), as they represent an improvement over previous conventional standards (e.g. Anders and Grevesse 1989; Grevesse et al. 2005, 2007) and result from the use of a 3D hydrodynamic model of the solar atmosphere, nonlocal thermodynamic equilibrium effects, and improved atomic and molecular data. The photospheric values are then converted to protosolar elemental abundance (see table footnote). The latter account for the effects of diffusion at the bottom of the convective zone on the chemical composition of the photosphere, together with the effects of gravitational settling and radiative accelerations. According to Asplund et al. (2009), the protosolar metal abundances relative to hydrogen can be obtained from the present-day values increased by +0.04 dex, i.e. ~11%, with an uncertainty of ±0.01 dex; the effect of diffusion on He is very slightly larger: +0.05 dex (±0.01) (dex stands for "decimal exponent," so that 1 dex=10; it is a commonly used

unit in astrophysics). Lodders et al. (2009) suggest a slightly larger correction of +0.061 dex for He and +0.053 dex for all other elements. Previously, Grevesse et al. (2005, 2007) used the same protosolar correction of +0.05 dex for all elements.

Figure 2.1 is based on protosolar correction to Asplund et al. (2009) photospheric abundances, while Table 2.1 lists planetary elemental enrichment factors also for Lodders et al. (2009) protosolar values. Whereas the difference between the enrichment factors based on Asplund et al. and Lodders et al. values is at most 10 to 15% for most elements, Asplund et al. estimate nearly 30% greater enrichment for Ar/H, compared to Lodders et al. (Table 2.1).

The difference in Jupiter's Ar enrichment factors based on Asplund et al. (2009) and Lodders et al. (2009) can be traced back largely to the choice of O/H employed by the two sets of authors. Because of their high excitation potentials, noble gases do not have photospheric spectral features; hence their solar abundances are derived indirectly. Asplund et al. (2009) infer solar Ar/H following the same procedure as Lodders (2008), i.e. by using, amongst other things, the Ar/O data from the solar wind, solar flares, and solar energetic particles, but employing their own photospheric abundances of O/H that have a somewhat lower uncertainty than Lodders et al. (2009). This accounts for much of the abovementioned 30% difference in Jupiter's Ar/H enrichment factor. Nevertheless, within the range of uncertainty of Jupiter's Ar abundance and the dispersion in the solar values, the Ar/H enrichment in Jupiter relative to the solar Ar/H is nearly the same whether one uses Asplund et al. (2009) or Lodders et al. (2009) solar Ar/H. We show both results in Figure 2.1. A word of caution about oxygen, which is used by the above authors as a proxy for deriving the solar Ar/H, is in order, however, as explained below.

Ever since concerted efforts were made to determine the solar elemental abundances, particular attention has been paid to oxygen, as oxygen is the most abundant element that was not created in the Big Bang, and third only to H and He, which were created in the Big Bang. Furthermore, the principal reservoir of oxygen in Saturn and Jupiter, H_2O, was presumably the original carrier of the heavy elements to these planets. Thus, oxygen is centrally important to the question of origin of all things. Yet, its abundance in the sun has been revised constantly. As illustrated in Figure 2.2, the solar O/H values have gyrated up and down several times in the past four decades, starting with the classic work of Cameron (1973) to the present. The highest solar O/H value is the one recommended by Anders and Grevesse (1989), which remained the standard for a good fifteen years, only to be revised downward by nearly a factor of two in 2005 (Grevesse et al. 2005), and having crept up a bit since then. Not surprisingly, the solar Ar/H, also plotted in Figure 2.2, shows the same trend as O/H over time, though they are not completely proportional to each other, nor are they expected to be. Thus, one needs to be vigilant about changes in the photospheric abundance of oxygen and other elements such as argon that use oxygen as a reference.

In summary, the most robust elemental abundance determined to date in Saturn is that of carbon. At 9× solar, Saturn's C/H is a little over twice the C/H ratio in Jupiter. This is consistent with the core accretion model of giant planet formation, according to which progressively increasing elemental abundance ratios are expected from Jupiter to Neptune. Carbon is the only heavy element ever determined for all four giant planets (Figure 2.1), and indeed it is found to increase from 4× solar in Jupiter to 9× solar in Saturn, rising to 80(±20)× solar or greater in both Uranus (Sromovsky et al. 2011; E. Karkoschka and K. Baines personal communication, 2015) and Neptune (Karkoschka and Tomasko 2011), using the current solar C/H from Table 2.1. The same trend is also seen in the S/H ratio of Saturn compared to Jupiter, except for a fourfold increase from Jupiter to Saturn, but Saturn's S/H is less secure, as discussed above. The difference in the relative changes of C/H and S/H is worth noting, but caution should be exercised to not overinterpret it. This is because H_2S is a thermochemically condensible volatile in the gas giants, unlike CH_4. Saturn's S/H would benefit greatly from a fresh set of modern data. A similar fourfold increase is also seen in the P/H ratio in Saturn compared to that in Jupiter, and the relative change may be valid if the disequilibrium species PH_3 meets a similar fate in the tropospheres of Saturn and Jupiter. On the other hand, the observed 3× solar N/H ratio in Saturn seems puzzling, as it is about a factor of two less, not more, than Jupiter's N/H, contrary to the predictions of conventional formation models. However, the